Molecular Crystals and Liquid Crystals

Publication details, including instructions for authors and subscription information:
http://www.tandfonline.com/loi/gmcl20

3-D OPTICAL SIMULATIONS OF AZIMUTHAL BISTABLE NEMATIC DEVICES

Emmanouil E. Kriezis [a], Steve J. Elston [a], Christopher J. Newton [b] & Timothy P. Spiller [b]

[a] University of Oxford, Department of Engineering Science, Oxford OX1 3PJ, United Kingdom

[b] Hewlett-Packard Laboratories, Filton Road Stoke Gifford, Bristol BS34 8QZ, United Kingdom

Version of record first published: 07 Jan 2010

To cite this article: Emmanouil E. Kriezis, Steve J. Elston, Christopher J. Newton & Timothy P. Spiller (2004): 3-D OPTICAL SIMULATIONS OF AZIMUTHAL BISTABLE NEMATIC DEVICES, Molecular Crystals and Liquid Crystals, 413:1, 321-331

To link to this article: http://dx.doi.org/10.1080/15421400490437042

Mol. Cryst. Liq. Cryst., Vol. 413, pp. 321/[2457]–331/[2467], 2004

ISSN: 1542-1406 print/1563-5287 online
DOI: 10.1080/15421400490437042

Taylor & Francis
Taylor & Francis Group

3-D OPTICAL SIMULATIONS OF AZIMUTHAL BISTABLE NEMATIC DEVICES

Emmanouil E. Kriezis and Steve J. Elston
University of Oxford, Department of Engineering Science
Oxford OX1 3PJ, United Kingdom

Christopher J. Newton and Timothy P. Spiller
Hewlett-Packard Laboratories, Filton Road Stoke Gifford,
Bristol BS34 8QZ, United Kingdom

A composite scheme based on the Finite-Difference Time-Domain (FDTD) method and a plane wave expansion is developed and applied to the optics of doubly periodic liquid crystal microstructures. This is used to investigate 3-D light wave propagation in grating aligned azimuthal bistable nematic devices.

Keywords: azimuthal bistable nematic devices; FDTD method; wave propagation

INTRODUCTION

Bistable liquid crystal devices are currently of significant technological interest for low-power display applications. One method of obtaining bistability is to use a surface relief grating with a grating pitch of around one micron. Devices based on mono-gratings and doubly periodic surface relief gratings have been reported [1,2]. To characterise and optimise the optical properties of such devices one needs an optical model that will handle these surface relief gratings. We show that classical approaches for optical calculations, as based on the Extended Jones or the Berreman methods, combined with some kind of director averaging over the transverse directions introduce significant errors for practical device calculations. In any case, these methods do not generate any information about diffractive

EEK acknowledges the financial support of the HP Laboratories, Bristol and the Royal Society.

Address correspondence to Emmanouil E. Kriezis, University of Oxford, Department of Engineering Science, Oxford, OXI 3PJ, United Kingdom.

effects and these may be important. This work introduces a rigorous 3-D model of optical wave propagation that can be used to accurately model such LC devices.

The model uses the Finite-Difference Time-Domain (FDTD) method [3–6] for the region of the device that involves 3-D variations in geometry, and uses plane wave expansions for the lower and upper supporting layer stacks (which are uniform along both transverse directions and very thick compared to the LC layer). This hybrid approach greatly reduces the computational burden and allows for realistic devices to be easily modelled.

Detailed models of realistic devices are analysed with emphasis on two different underlying double-periodic surface relief gratings for azimuthal bistable nematic (ABN) operation: a smooth bi-sinusoidal (BS) grating and a square-post (SP) array. The influence of the grating feature size on the direct and diffracted portion of light is quantified. Device performance is examined in conjunction with an appropriate compensation layer, and the optimum layer thickness is determined for the different grating geometries.

DESCRIPTION OF THE WAVE PROPAGATION SCHEME

A cross-section of a typical transmissive bistable nematic device is shown in Figure 1. One of the supporting surfaces has a relief type grating with double periodicity along the axes $\hat{x}$ and $\hat{y}$ and pitch lengths (P_x, P_y) in the order of a micron. The LC material will exhibit periodic director ($\hat{n}$) orientation with significant variation along all three spatial directions and the same is also true for the optical dielectric tensor ($\tilde{\varepsilon}$):

$$\hat{n}(x+P_x,y+P_y,z)=\hat{n}(x,y,z)\ ;\ \tilde{\varepsilon}(x+P_x,y+P_y,z)=\tilde{\varepsilon}(x,y,z) \qquad (1)$$

As the optical tensor variation is on the optical wavelength scale, a rigorous treatment of light wave propagation inside the LC material will require true consideration of the 3-D optical tensor variation.

The average LC layer thickness required for the birefringence of commonly available nematic materials is usually in the order of 2–4 μm with the grating depth being typically less than a micron. Therefore, the combined LC and grating thickness are just few microns and encompasses all the 3-D variation in optical properties. Layers found above and below the combined LC and grating structure, such as the substrate, superstrate, entrance polariser, analyser and possibly some compensation layers are all uniform isotropic or anisotropic slabs without any lateral (x,y) variation. A thickness of hundreds of microns is typical for these stacks of layers preventing a unified numerical modelling based on a method requiring sub-wavelength spatial discretisation (such as the FDTD method).

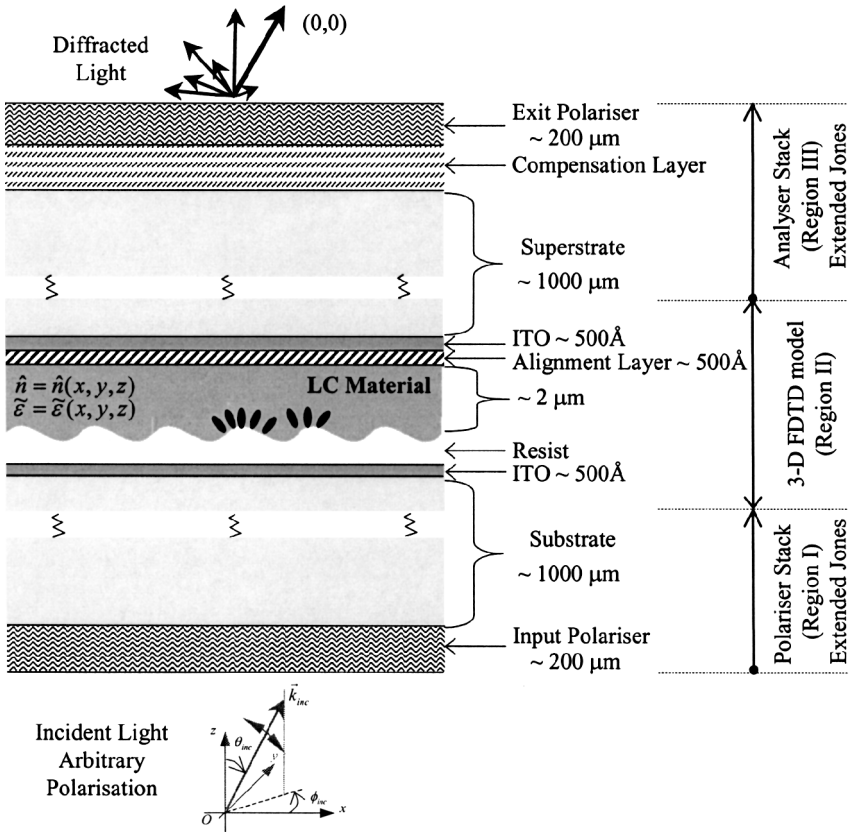

FIGURE 1 Typical cross-section of a bistable nematic device.

An effective approach is to split the problem space into three computational regions, marked as Region I, II and III in Figure 1, and then apply a suitable method in each of them.

Region II accommodates the LC material together with the grating structure, and it extends up to a limited depth inside the substrate and the superstrate. Variation of the optical tensor along all three spatial directions in this region is consistently taken into consideration by formulating light propagation in terms of Maxwell's equation in 3-D. Solution of Maxwell's equations is accomplished by the FDTD method, without the introduction of any approximations, apart from the numerical discretisation. Details on the FDTD implementation can be found in the literature [3–6].

Region I and III are stacks of uniform layers and propagation through them can be effectively modelled in the spectral-domain using one of the available methods for stratified-media optics, such as the Extended Jones

method [7]. Coupling between the FDTD method and the Extended Jones will be performed along two fictitious interfaces.

The composite scheme developed for light wave propagation studies inside the device depicted in Figure 1 consists of four steps. In the first step an arbitrary plane wave is assumed to illuminate the device. The propagation of this wave is traced through Region I by the application of the Extended Jones method until the interface with Region II. In the second step, the already determined expression for the plane wave along the interface is used as the excitation of the 3-D FDTD grid. The main numerical burden of the scheme resides in this step, with the FDTD simulation continuing until the fields in Region II reach their steady state. The third step involves a decomposition of the forward propagating field over the interface between Region II/Region III into a discrete plane wave spectrum, and then the tracing of each wave through the layers of the analyser stack (Region III) by the Extended Jones method. Completion of this step will yield the transmitted optical wave, in the form of a discrete plane wave spectrum. The fourth step is similar to the third step and it involves decomposition of the backward-propagating field over the interface between Region I/ II into a wave spectrum. Subsequently, this spectrum will now be passed through the layers of the entrance stack (Region I), which are now presented in reverse order. Further details on the implementation of this composite scheme have been reported elsewhere [5].

NUMERICAL APPLICATIONS

We will consider two different grating geometries: a smooth bi-sinusoidal (BS) grating (Fig. 2a) and an array of square posts (SP) (Fig. 2b). For

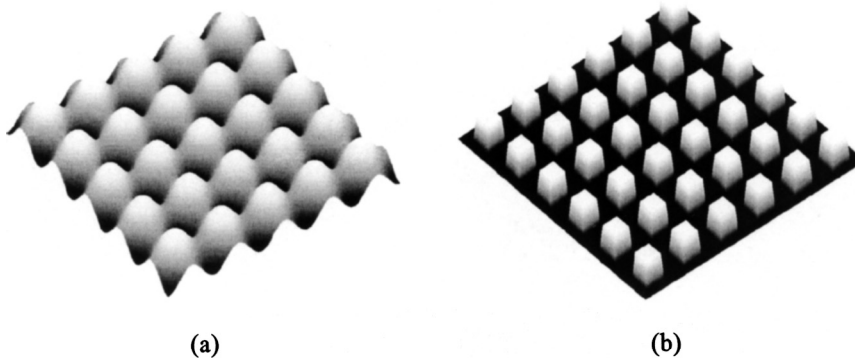

FIGURE 2 (a) Bi-sinusoidal grating; (b) Square post array.

the BS grating the boundary is represented by the expression

$$z(x,y) = \frac{F}{4}\left[-2 + \cos\left(\frac{2\pi x}{P_x}\right) + \cos\left(\frac{2\pi y}{P_y}\right)\right] \tag{2}$$

with factor F controlling the feature size. In the case of the SP array the post height is fixed and equal to F with a cross-sectional boundary defined by:

$$\left(x - \frac{P}{2}\right)^6 + \left(y - \frac{P}{2}\right)^6 = \left(\frac{P}{4}\right)^6; \quad P = P_x = P_y \tag{3}$$

For practical applications a common pitch along $\hat{x}$ and $\hat{y}$ directions has been considered ($P_x = P_y = 1.4\,\mu\text{m}$), in conjunction with feature sizes of $F = 300{,}400{,}500\,\text{nm}$.

Liquid Crystal orientation profiles have been obtained for the above 3D structures using a free energy minimisation technique [8]. This minimises the sums of the volume integrals of the bulk distortion energy and the surface energy. Simulations have been performed on a 50 nm cubic grid, under a single elastic constant approximation. The LC layer thickness was 2 μm when measured from the grating troughs to the upper flat boundary. Strong planar alignment was used on both surfaces. For the SP array two stable states are found corresponding to an ABN structure. One state is aligned mainly along the line $y = x$ with the other aligning mainly along $y = -x$. In the BS grating case many stable states exist, as any azimuthal direction across the surface has the same energy. However, director profiles mainly aligned along the lines $y = x$ and $y = -x$ have been determined for meaningful comparisons.

Figure 3 illustrates the director orientation profiles obtained for both LC structures, with a typical feature size of $F = 400\,\text{nm}$. These discrete profiles are then used to generate the discrete optical tensor profiles.

In the absence of the grating structure and the associated distortion of the director orientation in the vicinity of the grating, one can estimate that the device will function approximately as a $3\pi/2$ uniform plate (more precisely 1.4π) with the optic axis oriented along $\phi = 45^\circ$ (when LC orientation is mainly along the line $y = x$) or $\phi = -45^\circ$ (when along $y = -x$), depending on the bistable state. Therefore, for display operation the device should be combined with a compensation layer close to a quarter-wave plate ($\lambda/4$ plate) oriented at 45°. Arranging the polariser at 0° and the analyser at 90° will result in the $\phi = 45^\circ$ state appearing dark (total retardation $\sim 2\pi$), whereas the $\phi = -45^\circ$ will appear bright (total retardation $\sim \pi$).

Departure from this idealised response occurs for a number of reasons. Firstly the presence of the grating results in diffraction, and therefore, at the exit side of the device light will emerge along discrete directions.

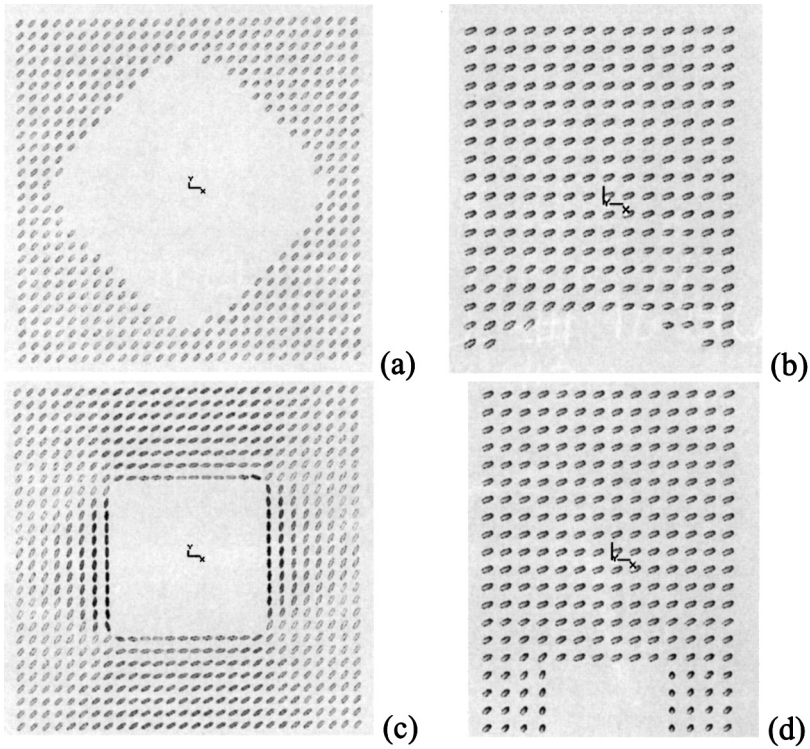

FIGURE 3 Director orientation for gratings with a 400 nm feature size: (a) BS, top-view; (b) BS, cross-section; (c) SP, top-view; (d) SP, cross-section.

Secondly, the grating structure distorts the LC orientation close to its surface, and thus the phase retardation introduced will strongly depend on the grating geometry and the extent/variation of LC orientation in the distortion zones. This means that the thickness of the compensation layer must be tailored for different gratings to observe optimum performance. Moreover, it is expected that the compensation layer will *not* in general act in the same way on the directly transmitted (0th order) light and on the diffracted (higher orders) light. For instance, a particular compensation layer might extinguish the 0th order in the dark state but still some light may leak through due to higher orders, thus reducing the contrast ratio (CR) in particular directions.

Figure 4 shows the 0th order and total transmitted power versus a compensation layer thickness for both grating structures illuminated at normal incidence with a free space wavelength of 650 nm. The compensation layer considered is a uniform anisotropic slab with the optic axis aligned along

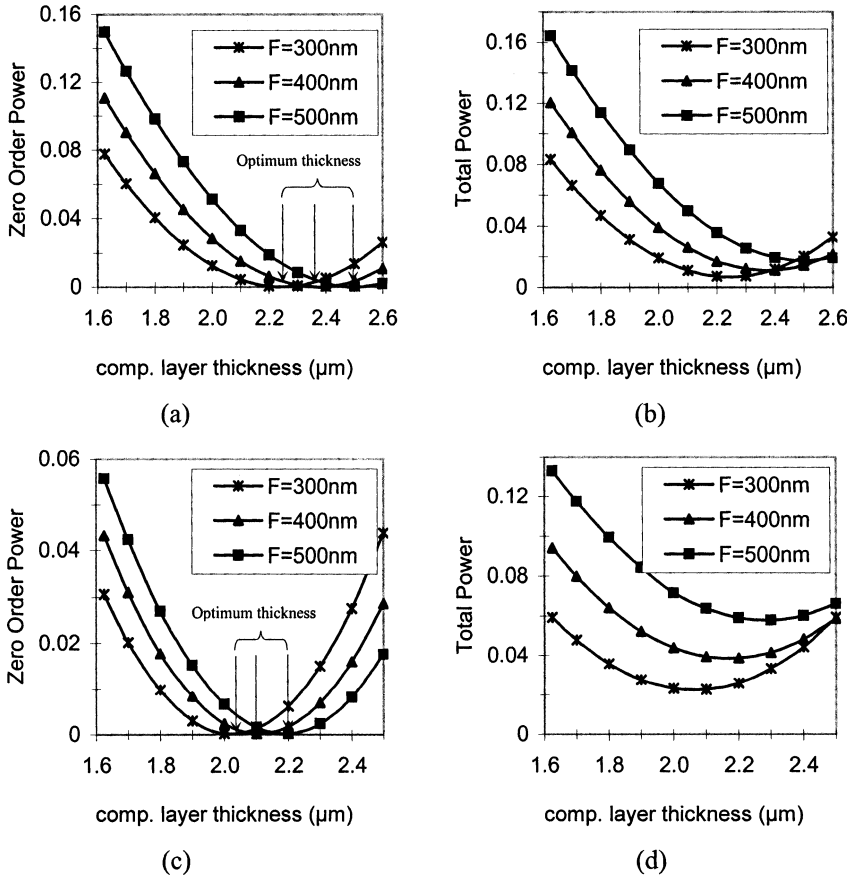

FIGURE 4 Normalised transmitted power for the dark state – effect of feature size. (a) BS, 0th order power; (b) BS, total power; (c) SP, 0th order power; (d) SP, total power.

45° and birefringence $\Delta n = 0.1$. The graphs correspond to the dark state ($\phi = 45°$). It can be seen that the 0th order light can be completely extinguished for a suitable compensation layer thickness, and the particular thickness required strongly depends on the feature size, as clearly marked on Figure 4a and 4c. Gratings with increased feature size require a thicker compensation layer in order to cancel out the 0th order. At this compensation layer thickness light is only carried by the higher diffracted orders and for the BS geometry this can be around 0.7–1.7% of incident light, depending on the grating feature size (Fig. 4b). The corresponding total transmitted power for the square post array goes through a global minimum in the vicinity of the 0th order null, but now the remaining light power in

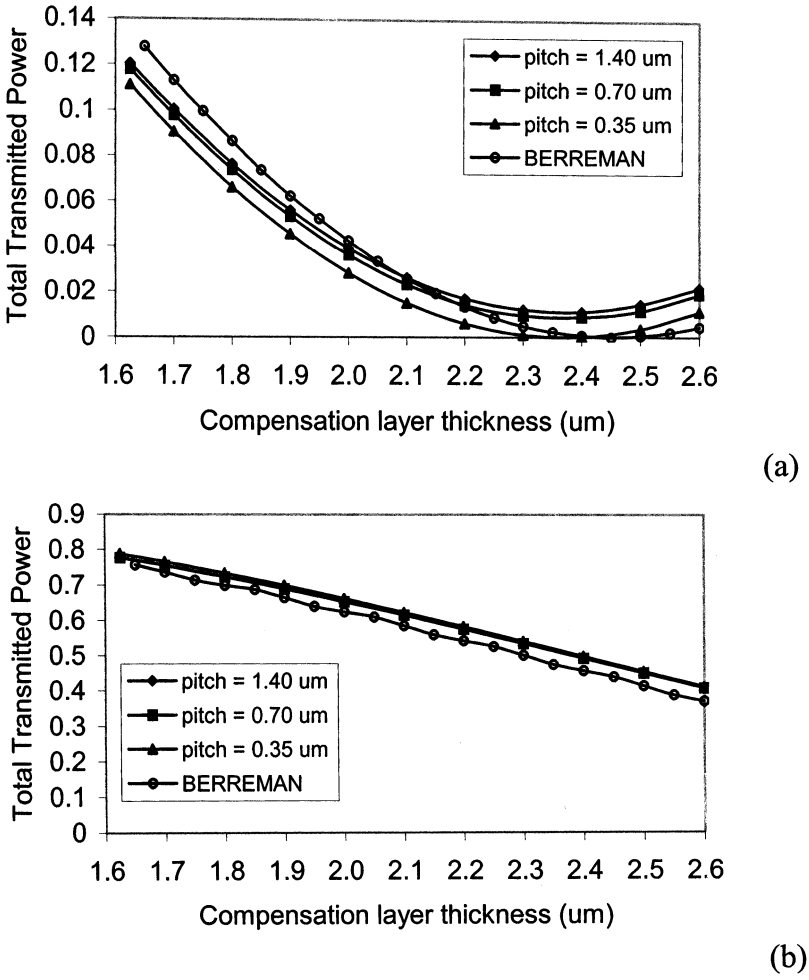

FIGURE 5 Normalised total transmitted power–effect of lateral pitch. (a) BS, dark state; (b) BS, bright state; (c) SP, dark state; (d) SP, bright state.

the higher order modes is in the region of 2.2–5.8% (Fig. 4d), still strongly dependent on the feature size. These much higher values compared to the BS case are clearly expected, as the SP array is far more diffractive. It is evident that this light leakage will degrade the CR.

One obvious way to suppress the diffractive effects is to reduce the device lateral pitch. As the lateral pitch is reduced less diffraction orders are propagating and at some point only the 0th order mode will be left with all higher orders being evanescent. For an appropriate compensation layer

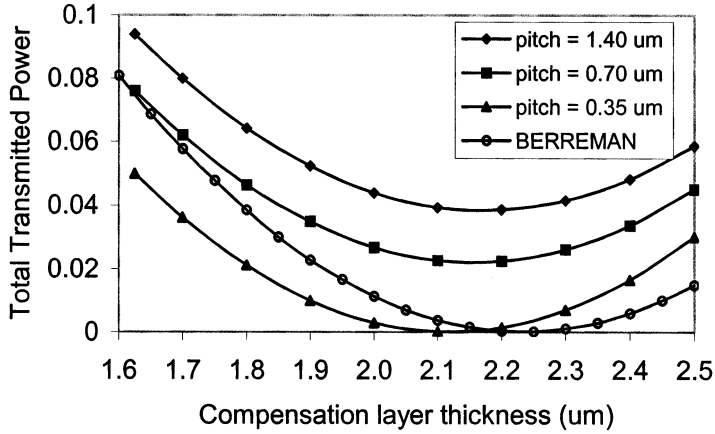

(c)

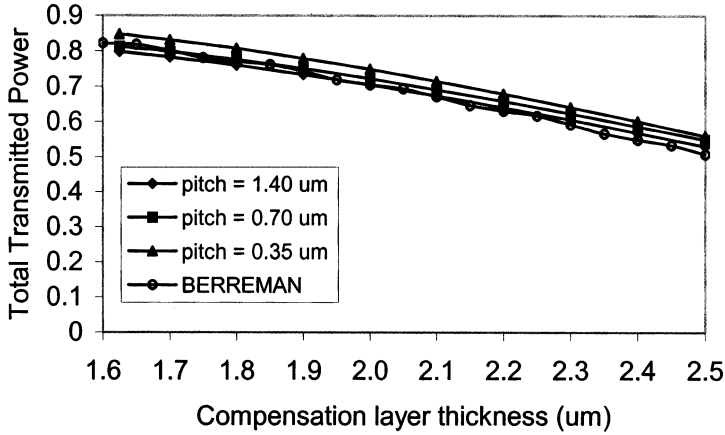

(d)

FIGURE 5 (Continued).

this leads to perfect extinction now of the total transmitted light enhancing the CR. If strong LC anchoring is assumed then the director profiles will effectively remain the same under this compression of lateral dimensions. Unfortunately, this pitch reduction up to the point where all higher diffracted orders are evanescent is very likely to correspond to gratings with impractical dimensions for present technology applications.

Figure 5 demonstrates the influence of the lateral pitch (1.4 μm, 0.7 μm, 0.35 μm) for a fixed feature size of 400 nm. Both grating types are analysed in association with their dark and bright state. Reduction of the grating

pitch clearly improves the dark state, allowing also for light extinction, and at the same time it also increases the bright state transmittance. It is interesting to examine if under any conditions the Berreman method [9] can provide an acceptable approximation to the optics of these devices. This is expected to work only in the limit of very small lateral pitch (compared to the optical wavelength). In this limit the light will sense an *"effective medium"*, and therefore, averaging in the lateral direction in order to feed the Berreman method with a stratified approximation of the device should produce consistent results with our composite FDTD/plane wave scheme.

The Berreman prediction is included in Figure 5 and reasonably compares with the smallest pitch analysed (0.35 μm), which is just smaller compared to the optical wavelength measured inside the material. Better agreement will be reached if the lateral pitch is further reduced. However, such fine pitch sizes are well beyond any present technology and so more complex numerical modelling is necessary for accurate optical calculations. The small ripples seen in Figures 5b and 5d are due to multiple reflections from the air/glass interfaces, which are not modelled in our scheme, as we have used the Extended Jones to implement the polariser and analyser stacks.

CONCLUSIONS

We have proposed and demonstrated a rigorous numerical simulation of light wave propagation in 3-D realistic ABN LC devices by a combination of the FDTD method and the Extended Jones method. The supporting grating and the director orientation can be allowed to have any arbitrary variation in 3-D. Approximations have been kept to a bare minimum. Computational burden is high but is not a restrictive term. Reliable results can only be obtained using the Berreman method when the grating pitch is very small, way below what is currently realisable. For practical devices our combined scheme enables accurate calculations to be performed and device parameters to be optimised.

REFERENCES

[1] Brown, C. V., Bryan-Brown, G. P., & Hui, V. C. (1997). *Mol. Cryst. Liq. Cryst.*, *301*, 163.
[2] Bryan-Brown, G. P., Towler, M. J., Bancroft, M. S., & McDonnell, D. G. (1994). *Proceedings of International Display Research Conference* (IDRC'94), 209.
[3] Kriezis, E. E. & Elston, S. J. (2000). *Optics Com.*, *177*, 69.
[4] Kriezis, E. E., Filippov, S. K., & Elston, S. J. (2000). *J. Opt. A: Pure Appl. Opt.*, *2*, 27.
[5] Kriezis, E. E., Newton, C. J., Spiller, T. P., & Elston, S. J. (2002). *Appl. Optics.*, *41*, 5346.
[6] Taflove, A. & Hagness, S. C. (2000). *Computational Electrodynamics: The Finite-difference Time-domain Method*, Artech House: Boston.

[7] Gu, C. & Yeh, P. (1999). *Displays*, *20*, 237.
[8] Newton, C. J. & Spiller, T. P.(1997). *Proceedings of International Display Research Conference* (SID'97), 13.
[9] Berreman, D. W. (1972). *J. Opt. Soc. Am.*, *62*, 502.